ANS M&C 2021 - The International Conference on Mathematics and Computational Methods Applied to Nuclear Science and Engineering · Raleigh, North Carolina · October 3–7, 2021

MARKOVIAN BINARY MIXTURES: BENCHMARKS FOR THE ALBEDO PROBLEM

Coline Larmier[1], Eugene d'Eon[2], and Andrea Zoia[1]

[1]Université Paris-Saclay, CEA, Service d'études des réacteurs et de mathématiques appliquées, 91191, Gif-sur-Yvette, France

[2]NVIDIA
2788 San Tomas Expressway, Santa Clara, CA. 95050

coline.larmier@cea.fr, edeon@nvidia.com, andrea.zoia@cea.fr

ABSTRACT

We present new albedo-problem benchmarks for three-dimensional stochastic media. We use an unbiased Monte Carlo method to estimate the law of diffuse reflection for a binary Markov stochastic half-space with plane-parallel illumination at the boundary. These gold-standard quenched-disorder benchmarks are compared to four annealed-disorder models: the atomic-mix (AM) approximation, the standard Chord-Length Sampling (CLS) method, and two distinct proposals of Generalized Radiative Transfer (GRT) that apply the generalized linear Boltzmann equation in bounded domains. Across nine benchmarks (using isotropic scattering) we observe that memory effects can lead to significant errors in all four annealed models. For non-stochastic albedo, the reciprocal formulation of GRT is universally more accurate than the alternative proposal.

KEYWORDS: Non-classical transport, Binary mixtures, Albedo problem, Benchmark, BRDF

1. INTRODUCTION

Accurately predicting the linear transport of waves or particles in stochastic media is a challenging and important problem. One particular class of stochastic media, *Markovian binary mixtures* (MBMs), has a number of applications, such as shielding materials [1] and light transport in molecular clouds [2]. A convenient property of MBMs is that exact realizations can be efficiently generated in 3D [3]. Combined with Monte Carlo simulation, this enables the generation of quenched-disorder reference solutions, which can be used to evaluate the accuracy of approximate numerical methods for stochastic transport. In this paper we present new MBM benchmark solutions for the half-space albedo problem. Previous benchmarks for the external illumination of stochastic media have been limited to normal incidence and report only the scalar reflected and transmitted albedos [2–4]. In this work, we simulate a variety of illumination angles and report the full angular distribution at the boundary to investigate the law of diffuse reflection (bidirectional reflectance distribution function or BRDF), which is important for applications such as remote sensing and computer graphics.

The Monte Carlo quenched-disorder approach produces gold-standard reference solutions but has a high computational cost. This has motivated a number of approximate annealed-disorder models for describing transport in stochastic media that have comparable efficiency to standard methods for solving non-stochastic problems. We compare our benchmarks to four such models: a *Chord-Length-Sampling* (CLS) model consisting of Markov-renewal random flights, two *generalized radiative transfer* (GRT) models consisting of renewal random flights, and the *atomic-mix* (AM) approximation consisting of exponential random flights with homogenized parameters. We also expand upon prior quenched-disorder evaluations of the *generalized linear Boltzmann equation* (GLBE) [5], which were restricted to two-dimensions [6,7]. This is accomplished via the GRT results, whose angular fluxes satisfy the GLBE. In particular, we compare two proposals for applying the GLBE to bounded domains [6,7], which have different intercollision free-path-length statistics.

2. BENCHMARK SPECIFICATION

For each quenched-disorder benchmark, we computed mean observables over a sample of random realizations. In each realization, one of two phases (α or β) was stochastically assigned to positions in a 3D half space using an isotropic Poisson tessellation [3]. We repeated the three mixing statistics of the Adams, Larsen and Pomraning (ALP) benchmarks ("1", "2", and "3"), which vary the mean chord lengths $\Lambda_\alpha, \Lambda_\beta > 0$ and total macroscopic cross sections $\Sigma_\alpha, \Sigma_\beta \geq 0$ in each phase. Three different absorption configurations ("a", "b", and "c") were assigned to each class of mixtures for a total of nine benchmarks configurations. In the "a" and "b" cases, one phase is purely scattering and the other purely absorbing. In the "c" cases, the single-scattering albedo is a non-stochastic value, $c = 0.9$. Isotropic scattering was assigned to both phases in all benchmarks. We refer the reader to [3] for further details.

To approximate a semi-infinite half space, the lateral dimensions of a box were fixed at $L_y = L_z = 10$, and the depth extended to emulate an optically-thick half space ($L_x = 20$ for case 1 and $L_x = 200$ for cases 2 and 3). Mirror boundaries were applied on the four sides of the box and vacuum boundary conditions on the illuminated face and its opposing face. The number of sampled realizations was 500 for case 1, 10000 for case 2 and 20000 for case 3. We simulated 10^7 particle histories in each realization using standard Monte Carlo methods. The box was subject to unidirectional deterministic illumination distributed uniformly over a square of unit width centered on the face located at $x = 0$. Four illumination directions with cosines $\mu_0 \in \{1, 0.7, 0.5, 0.3\}$ were simulated per benchmark. The angular flux of the boundary source was scaled by $1/\mu_0$ so that the integrated emerging distribution gives the albedo directly. The maximum observed transmitted leakage from the $x = L_x$ face was 0.00056 (case 1c), which ensures that the optical thickness along the x axis was sufficient for our purposes.

Observables For each illumination condition we tallied the azimuthally-integrated emerging angular flux $\psi(0, \mu)$ at the illuminated face located at $x = 0$ (including separate tallies for the single-scattered $\psi_1(0, \mu)$ and doubly-scattered $\psi_2(0, \mu)$ components). By this definition, $\psi(0, \mu)\mu d\mu$ is the probability that a particle entering the box with cosine μ_0 eventually escapes the medium along a direction with cosine in $[\mu, \mu + d\mu]$. The BRDF then follows from $f_r(\mu, \mu_0) = \psi(0, \mu; \mu_0)/(2\pi)$ due to the isotropic scattering removing all azimuthal dependence. We also report the total diffuse albedo of the material,

$$R(\mu_0) = \int_0^1 \psi(0,\mu)\mu d\mu. \tag{1}$$

The collision densities $C(x)$ at depth x were also tallied, defined such that $C(x)dx$ is the expected number of times a particle collides in $[x, x+dx]$ before either being absorbed or escaping.

Validation To validate our implementation, we verified that the collision density of the particle's first collision matched the density that follows from the Levermore-Pomraning attenuation law, which is an exact result for MBMs [8] that we recall here. The *volume fractions* in each phase

$$v_i = \frac{\Lambda_i}{\Lambda_\alpha + \Lambda_\beta}, \quad i = \alpha, \beta \tag{2}$$

give the *mean total cross section* $\langle\Sigma\rangle = v_\alpha\Sigma_\alpha + v_\beta\Sigma_\beta$ and two auxiliary quantities

$$\tilde{\Sigma} = v_\beta\Sigma_\alpha + v_\alpha\Sigma_\beta + \Lambda_\alpha^{-1} + \Lambda_\beta^{-1} \tag{3}$$

$$\gamma = (\Sigma_\alpha - \Sigma_\beta)^2 v_\alpha v_\beta. \tag{4}$$

The hyperexponential distributions that characterize Markov binary mixtures share two common decay constants [9,8]

$$2r_\pm = \langle\Sigma\rangle + \tilde{\Sigma} \pm \sqrt{\left(\langle\Sigma\rangle - \tilde{\Sigma}\right)^2 + 4\gamma}. \tag{5}$$

We further define the weights $w_\pm$ of the two exponentials as

$$w_+ = \frac{\tilde{\Sigma} - r_-}{r_+ - r_-}, \quad w_- = 1 - w_+. \tag{6}$$

With these, we can express the attenuation law from a deterministic (equilibrium) origin as [8]

$$X_u(s) = w_- e^{-r_- s} + w_+ e^{-r_+ s}, \tag{7}$$

where $X_u(s)$ is the mean probability of experiencing no collisions when traversing a free-path of length s from the boundary. Under the present assumption of isotropic stochastic media, these statistics are invariant to the direction of the free path. The density $p_u(s)$ of the distance s to the first collision in the medium is a related hyperexponential [10,7,11]

$$p_u(s) = w_- r_- e^{-r_- s} + w_+ r_+ e^{-r_+ s}, \tag{8}$$

which was used to test our simulations for all medium configurations and illumination angles. We also verified that the emerging distribution and total diffuse albedo of our benchmark implementation matched Chandrasekhar's exact solution (recalled in Section 3.3) when identical cross sections and albedos were assigned to both phases ($\Sigma_\alpha = \Sigma_\beta, c_\alpha = c_\beta$).

3. APPROXIMATE TRANSPORT MODELS

We compared our quenched disorder simulations to four approximate transport models, each comprising a random flight in 3D with isotropic scattering. These models differ in the probability densities and related particle states used to sample free-path lengths and determine absorption probabilities. We review the details of these random flights in this section.

3.1. Chord-Length Sampling (CLS)

The standard CLS algorithm for Markov media ([3], algorithm A) simulates the particle history using a random flight with an additional state variable i that tracks the current phase. The phase is initialized at the boundary by sampling from the discrete (equilibrium) distribution with probabilities $\{v_\alpha, v_\beta\}$ (Eq.(2)). Each free-path length of the random flight is then sampled by determining a free-path length in the current phase (using Σ_i) and a partial chord-length to the next phase transition (using Λ_i) and selecting the minimum of the two distances. In the latter case, the phase state i is swapped and the particle continues forward in the null-collision sense.

Because the CLS flight depends only on the current phase and not the rest of the particle history, this is tantamount to assuming that the arrival times of the real collisions are exactly those times that follow from the particle undergoing purely forward scattering along a transect through an infinite Markov binary mixture. The Cox / doubly-stochastic Poisson process producing these times is modulated by a dichotomic Markov process (the alternating renewal process giving the phase transitions along the transect), which results in a Markov-modulated Poisson process (MMPP). This is known to reduce to a Markov renewal process for the arrival times [12]. Thus, the inter-collision lengths can be sampled in a single step (avoiding the null collisions) using the two-state Markov-renewal statistics [12]

$$p_{ij}(x) = \begin{pmatrix} \frac{\Sigma_\alpha e^{-r^+ x}(-\frac{1}{\Lambda_\beta}+r^+-\Sigma_\beta)}{r^+-r^-} + \frac{\Sigma_\alpha e^{-r^- x}(\frac{1}{\Lambda_\beta}-r^-+\Sigma_\beta)}{r^+-r^-} & \frac{\frac{1}{\Lambda_\alpha}\Sigma_\beta\left(e^{-r^- x}-e^{-r^+ x}\right)}{r^+-r^-} \\ \frac{\frac{1}{\Lambda_\beta}\Sigma_\alpha\left(e^{-r^- x}-e^{-r^+ x}\right)}{r^+-r^-} & \frac{\Sigma_\beta e^{-r^+ x}(-\frac{1}{\Lambda_\alpha}+r^+-\Sigma_\alpha)}{r^+-r^-} + \frac{\Sigma_\beta e^{-r^- x}(\frac{1}{\Lambda_\alpha}-r^-+\Sigma_\alpha)}{r^+-r^-} \end{pmatrix} \tag{9}$$

where $p_{ij}(x)$ is the probability density of leaving phase i and colliding in phase j after a free-flight of length x.

In the case of a Dirac (purely-forward) scattering kernel, this CLS model exactly matches the quenched-disorder transport and should become increasingly accurate as the mean cosine of scattering approaches 1. For the present work, however, we limit the scope to isotropic scattering for the sake of conciseness. For the numerical CLS results, we performed Monte Carlo simulations in semi-infinite slabs with the same thickness L_x as the quenched benchmark simulations. We validated this implementation against exact semi-analytic solutions for the half space, which are possible to derive and will be presented in a future paper.

3.2. Generalized Radiative Transfer (GRT)

A number of stochastic transport processes have been proposed that generalize the exponential random flights of radiative transfer while maintaining the renewal character of the free-path lengths. This is achieved by adopting a non-exponential density $p_c(s)$ for distances s between collisions, thereby exhibiting spatial correlation and non-Beerian attenuation. Here, the label "c" denotes that this density is *conditional* (upon leaving a collision), as opposed to the statistics $p_u(s), X_u(s)$, which are *unconditional* (uniformly averaged over all realizations). The single-scattering albedo c and the phase function are assumed to be non-stochastic. Any memory effects beyond the two-point statistics between collisions are assumed negligible. The resulting process is therefore Markovian at the collision events and the integral equation for the collision density $C(x)$ is a generalization of Peierls', with the exponential kernel replaced by $p_c(s)$ [13]. In the case of isotropic scattering, this produces

$$C(\mathbf{x}) = C_0(\mathbf{x}) + c \iiint C(\mathbf{x}') \frac{p_c(|\mathbf{x}-\mathbf{x}'|)}{4\pi|\mathbf{x}-\mathbf{x}'|^2} d\mathbf{x}', \tag{10}$$

where $C_0(x)$ is the rate density of initial collisions. This form of non-classical transport is attractive in that it leads to Monte Carlo and deterministic methods that have a form and computational complexity similar to the classical case [14,11], requiring no additional state. Note that Eq.(10) is equivalent to the generalized linear Boltzmann equation (GLBE) (see [5], Eqs.(5.12)). We use the label "GRT", following Davis [15], to refer to these two equivalent formulations.

For bounded domains, two distinct forms of GRT have been proposed. In both, the mean attenuation law $X_u(s)$ from equilibrium (Equation 7 for Markov binary mixtures) is used to derive the mean density of free-path lengths $p_u(s)$ for the first collision from a deterministic origin (the boundary), $p_u(s) = -(\partial/\partial s)X_u(s)$, which determines $C_0(x)$. Several authors have proposed also using the equilibrium free-path statistics between collisions ($p_c(s) = p_u(s)$) to form an ordinary renewal process for all free-path lengths. This has been proposed for Markov binary mixtures [16,10,7] but is inconsistent with the stationarity of Σ and results in a non-reciprocal GRT theory [17]. Audic and Frisch [4] explain why the two distributions are different and propose a form of GRT with $p_c(s) \neq p_u(s)$, where $p_c(s)$ is estimated by Monte Carlo simulation in quenched disorder. Alternatively, the unique density $p_c(s)$ that ensures a stationary point process for the collision times and a transport model that satisfies Helmholtz reciprocity is given by the Palm-Kinchin equations for an equilibrium renewal process ([18], p.73), resulting in [6,11]

$$p_c(s) = \frac{1}{\langle\Sigma\rangle} \frac{\partial^2}{\partial s^2} X_u(s) = \frac{w_- r_-^2 e^{-r_- s} + w_+ r_+^2 e^{-r_+ s}}{\langle\Sigma\rangle}. \tag{11}$$

The Wiener-Hopf integral equation that follows from the plane-parallel projection of Eq.(10) can be solved by standard methods [11]. The resulting law of diffuse reflection for the reciprocal GRT model is

$$\begin{aligned}\psi(0,\mu) = \frac{c}{2} \Bigg[& r_+ w_+ H^\star\left(\frac{\mu}{r_+}\right) \left(\frac{w_+ H^\star\left(\frac{\mu_0}{r_+}\right)}{u + \mu_0} + \frac{w_- r_- H^\star\left(\frac{\mu_0}{r_-}\right)}{r_-\mu + r_+\mu_0} \right) \\ & + r_- w_- H^\star\left(\frac{\mu}{r_-}\right) \left(\frac{w_- H^\star\left(\frac{\mu_0}{r_-}\right)}{\mu + \mu_0} + \frac{w_+ r_+ H^\star\left(\frac{\mu_0}{r_+}\right)}{r_-\mu_0 + r_+\mu} \right) \Bigg]\end{aligned} \tag{12}$$

with generalized H-function

$$H^\star(z) = \exp\left(\frac{z}{\pi} \int_0^\infty \frac{1}{1+z^2t^2} \log\left[\frac{1}{1 - c\,\tilde{K}_C(t)} \right] dt \right), \quad \mathrm{Re}\, z > 0 \tag{13}$$

in terms of the Fourier-transformed collision kernel in plane geometry

$$\tilde{K}_C(z) = \frac{1}{\langle\Sigma\rangle} \frac{w_- r_-^2 \tan^{-1}\left(\frac{z}{r_-}\right) + w_+ r_+^2 \tan^{-1}\left(\frac{z}{r_+}\right)}{z}. \tag{14}$$

The GRT models have several limitations—they lack the additional memory of the CLS approach and also assume non-stochastic albedo. In the general case, the single-scattering albedo in a binary mixture is a complex function of the free-path length s, and so is inconsistent with GRT. For example, from the boundary we find (using Eq.(9))

$$c_u(s) = \frac{c_\alpha(v_\alpha p_{\alpha\alpha}(x) + v_\beta p_{\beta\alpha}(x)) + c_\beta(v_\alpha p_{\alpha\beta}(x) + v_\beta p_{\beta\beta}(x))}{p_u(s)}. \tag{15}$$

While varying $c(s)$ can be easily included in GRT [13], for the present we consider only the standard form. For the "a" and "b" benchmarks with stochastic albedo, we use the atomic-mix albedo

$$\langle c \rangle = \frac{\langle \Sigma_s \rangle}{\langle \Sigma \rangle} = \frac{v_\alpha c_\alpha \Sigma_\alpha + v_\beta c_\beta \Sigma_\beta}{v_\alpha \Sigma_\alpha + v_\beta \Sigma_\beta} \tag{16}$$

(see [19, Table 3] for the corresponding ALP benchmark values).

When only one phase scatters ($c_\beta = 0$), the MMPP for the collision times of a particle moving along a transect through the material reduces to a renewal process [12], making GRT an exact result, suggesting that the reciprocal GRT model will be increasingly accurate as the phase function is forward-peaked and $c_\beta \to 0$. Sahni [20] has presented a related integral-equation formulation for the case $c_\beta = 0$ and isotropic scattering.

3.3. Atomic Mix (AM)

For completeness, we compare to the atomic-mix approximation that forms a homogenized classical medium using the ensemble-averaged materials coefficients [8]. For all test cases the mean total cross section is $\langle \Sigma \rangle = 1$ and the atomic-mix albedo is defined above. The law of diffuse reflection of a classical half space is a function of c and the illumination cosine μ_0 [21]

$$\psi(0, \mu) = \frac{c}{2} \frac{H(\mu)H(\mu_0)}{\mu + \mu_0} \tag{17}$$

in terms of the H-function

$$H(\mu) = \exp\left(\frac{-\mu}{\pi} \int_0^\infty \frac{1}{1 + \mu^2 k^2} \ln \left(1 - c\frac{\arctan k}{k} \right) dk \right). \tag{18}$$

4. BENCHMARK COMPARISONS

Figure 1 shows the emergent distributions for the 9 benchmark scenarios for each of the four illumination angles, plotting azimuthally-integrated angular flux/radiance $I(0, \mu)$ at the illuminated boundary. The first- and second-order contributions to the full emergent distribution are similarly compared in Figures 2 and 3. In these plots the GRT model is the reciprocal version. For the 1a, 1c and 3a benchmarks, the annealed models agree reasonably well with quenched reference solutions, with more error for the normally-illuminated condition $\mu_0 = 1$. The 1b benchmark clearly illustrates the benefit of the additional memory of the CLS method over the alternative approximations. In all other benchmarks, significant errors (up to 30%) are evident in the CLS model. The total albedos and relative errors are also summarized in Table 1, where we also include the non-reciprocal version of GRT. Figure 4 compares the mean scalar collision density at depth x for the nine benchmark configurations. In a follow-up work, it would be interesting to add the Poisson-Box sampling models (CLS + memory) to the comparisons [22].

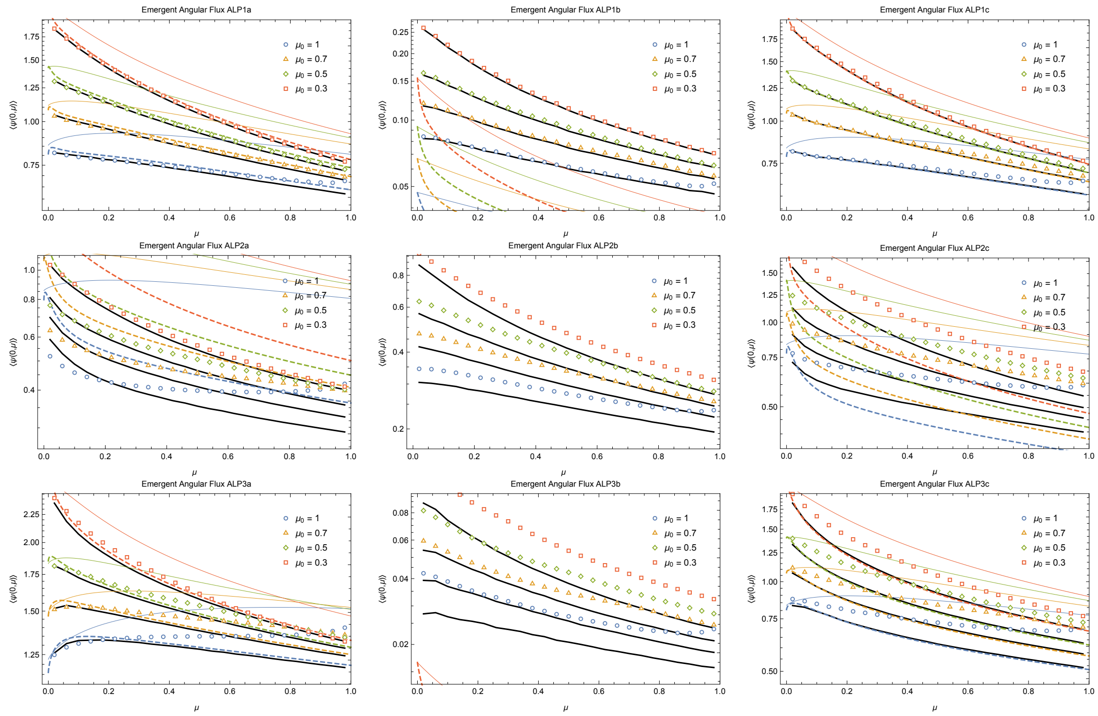

Figure 1: Azimuthally-integrated emergent flux benchmarks for collimated illumination with cosine μ_0—Quenched disorder (markers), CLS (black), GRT (dashed), AM (thin).

REFERENCES

[1] W. Burrus. "Radiation transmission through boral and similar heterogeneous materials consisting of randomly distributed absorbing chunks." Technical report, Oak Ridge National Lab., Tenn. (1960). URL https://doi.org/10.2172/4196641.

[2] P. Boissé. "Radiative transfer inside clumpy media-The penetration of UV photons inside molecular clouds." *Astronomy and Astrophysics*, **volume 228**, pp. 483–502 (1990).

[3] C. Larmier, A. Lam, P. Brantley, F. Malvagi, T. Palmer, and A. Zoia. "Monte Carlo chord length sampling for d-dimensional Markov binary mixtures." *Journal of Quantitative Spectroscopy and Radiative Transfer*, **volume 204**, pp. 256–271 (2018).

[4] S. Audic and H. Frisch. "Monte-Carlo simulation of a radiative transfer problem in a random medium: Application to a binary mixture." *Journal of Quantitative Spectroscopy and Radiative Transfer*, **volume 50**(2), pp. 127–147 (1993).

[5] E. W. Larsen and R. Vasques. "A generalized linear Boltzmann equation for non-classical particle transport." *Journal of Quantitative Spectroscopy and Radiative Transfer*, **volume 112**(4), pp. 619–631 (2011). URL https://doi.org/10.1016/j.jqsrt.2010.07.003.

[6] E. d'Eon. "A reciprocal formulation of nonexponential radiative transfer. 1: Sketch and motivation." *Journal of Computational and Theoretical Transport* (2018). URL https://doi.org/10.1080/23324309.2018.1481433.

[7] A. Frankel. "Solution of the Non-Classical Linear Boltzmann Equation for Transport in Multidimensional Stochastic Media." *Journal of Quantitative Spectroscopy and Radiative Transfer*, **volume 235**, pp. 60–69 (2019). URL https://doi.org/10.1016/j.jqsrt.2019.06.015.

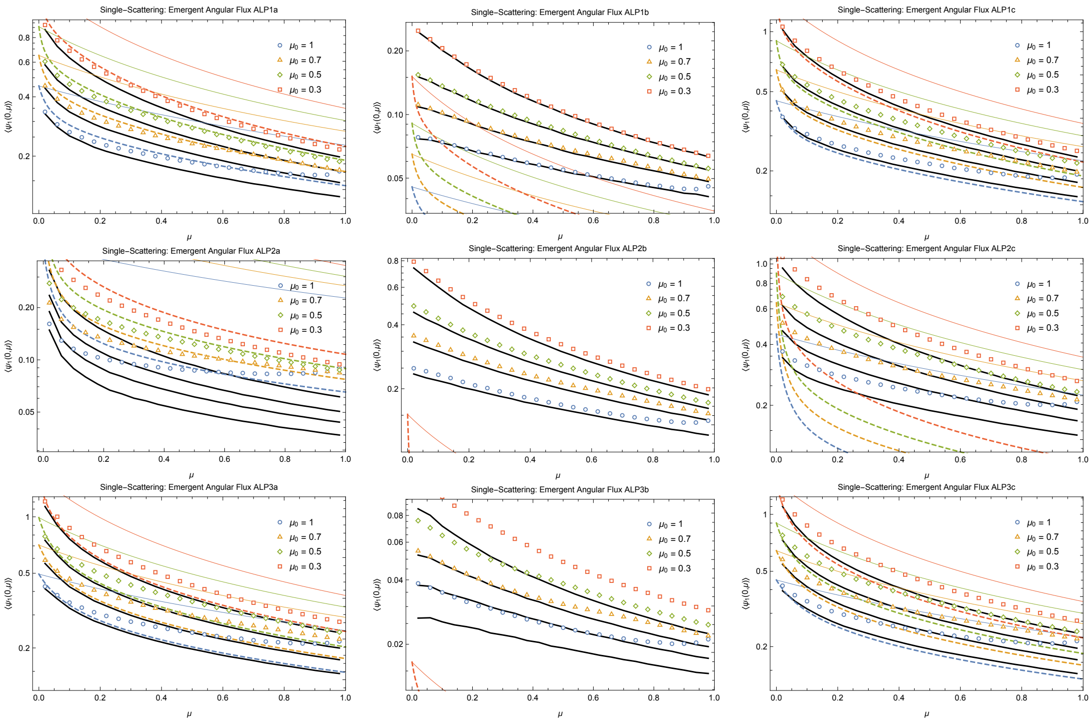

Figure 2: Once-scattered azimuthally-integrated emergent flux—Quenched disorder (markers), CLS (black), GRT (dashed), AM (thin).

[8] G. C. Pomraning. *Linear kinetic theory and particle transport in stochastic mixtures*, volume 7. World Scientific (1991).

[9] D. Gaver. "Random hazard in reliability problems." *Technometrics*, **volume 5**(2), pp. 211–226 (1963). URL https://doi.org/10.1080/00401706.1963.10490076.

[10] G. Glazov and G. Titov. "An integral equation for the average radiation intensity in a stochastically macroinhomogeneous medium." *Soviet Physics Journal*, **volume 20**(9), pp. 1204–1208 (1977). URL https://doi.org/10.1007/BF00897130.

[11] E. d'Eon. "The Albedo Problem in Nonexponential Radiative Transfer." *(ICTT-26)* (2019). URL https://www.researchgate.net/publication/333325137.

[12] W. Fischer and K. Meier-Hellstern. "The Markov-modulated Poisson process (MMPP) cookbook." *Performance evaluation*, **volume 18**(2), pp. 149–171 (1993).

[13] C. Grosjean. "The Exact Mathematical Theory of Multiple Scattering of Particles in an Infinite Medium." *Memoirs Kon Vl Ac Wetensch*, **volume 13**(36) (1951).

[14] E. d'Eon. "A reciprocal formulation of nonexponential radiative transfer. 2: Monte-Carlo Estimation and Diffusion Approximation." *Journal of Computational and Theoretical Transport*, **volume 48**(6), pp. 201–262 (2019). URL https://doi.org/10.1080/23324309.2019.1677717.

[15] A. B. Davis, F. Xu, and D. J. Diner. "Generalized radiative transfer theory for scattering by particles in an absorbing gas: Addressing both spatial and spectral integration in multi-angle remote sensing of optically thin aerosol layers." *Journal of Quantitative Spectroscopy and*

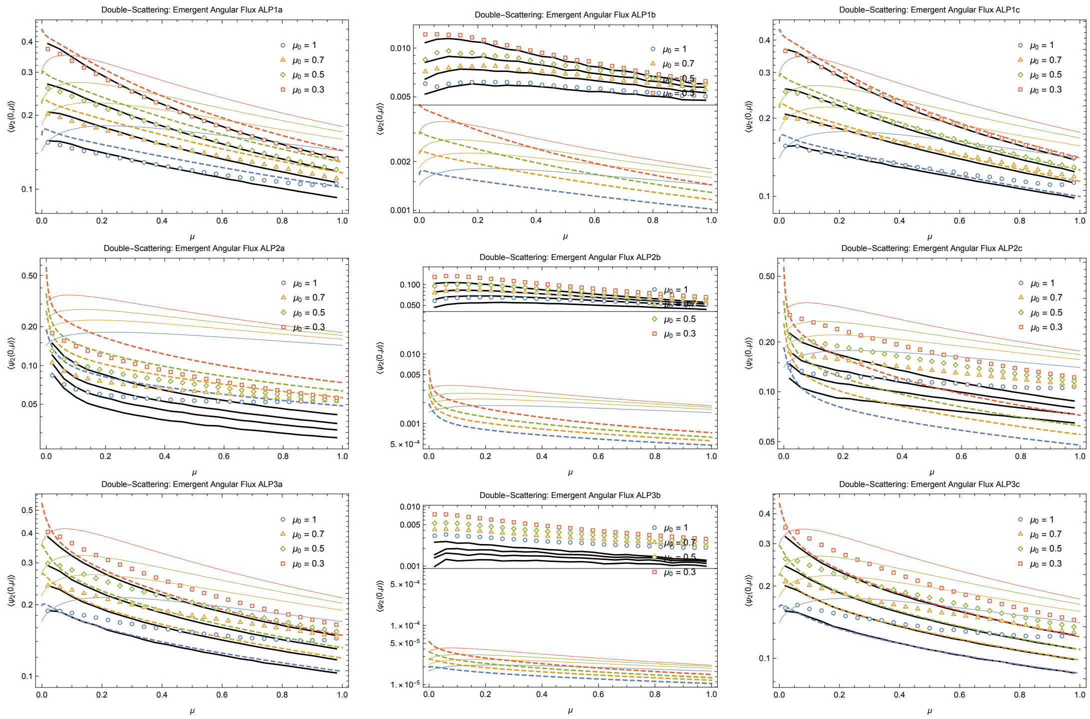

Figure 3: Twice-scattered azimuthally-integrated emergent flux—Quenched disorder (markers), CLS (black), GRT (dashed), AM (thin).

Radiative Transfer, **volume 205**, pp. 148–162 (2018). URL https://doi.org/10.1016/j.jqsrt.2017.10.003.

[16] O. Avaste and G. Vaynikko. "Solar radiation transfer in broken clouds." *Academy of Sciences, USSR, Izvestiya, Atmospheric and Oceanic Physics*, **volume 10**, pp. 645–649 (1974).

[17] A. B. Davis and F. Xu. "A generalized linear transport model for spatially correlated stochastic media." *Journal of Computational and Theoretical Transport*, **volume 43**(1-7), pp. 474–514 (2014). URL https://doi.org/10.1080/23324309.2014.978083.

[18] D. R. Cox and V. Isham. *Point processes*, volume 12. CRC Press (1980).

[19] C. Larmier, F.-X. Hugot, F. Malvagi, A. Mazzolo, and A. Zoia. "Benchmark solutions for transport in d-dimensional Markov binary mixtures." *Journal of Quantitative Spectroscopy and Radiative Transfer*, **volume 189**, pp. 133–148 (2017).

[20] D. Sahni. "Equivalence of generic equation method and the phenomenological model for linear transport problems in a two-state random scattering medium." *Journal of mathematical physics*, **volume 30**(7), pp. 1554–1559 (1989). URL https://doi.org/10.1063/1.528288.

[21] S. Chandrasekhar. *Radiative Transfer*. Dover (1960).

[22] C. Larmier, A. Zoia, F. Malvagi, E. Dumonteil, and A. Mazzolo. "Poisson-Box Sampling algorithms for three-dimensional Markov binary mixtures." *Journal of Quantitative Spectroscopy and Radiative Transfer*, **volume 206**, pp. 70–82 (2018). URL https://doi.org/10.1016/j.jqsrt.2017.10.020.

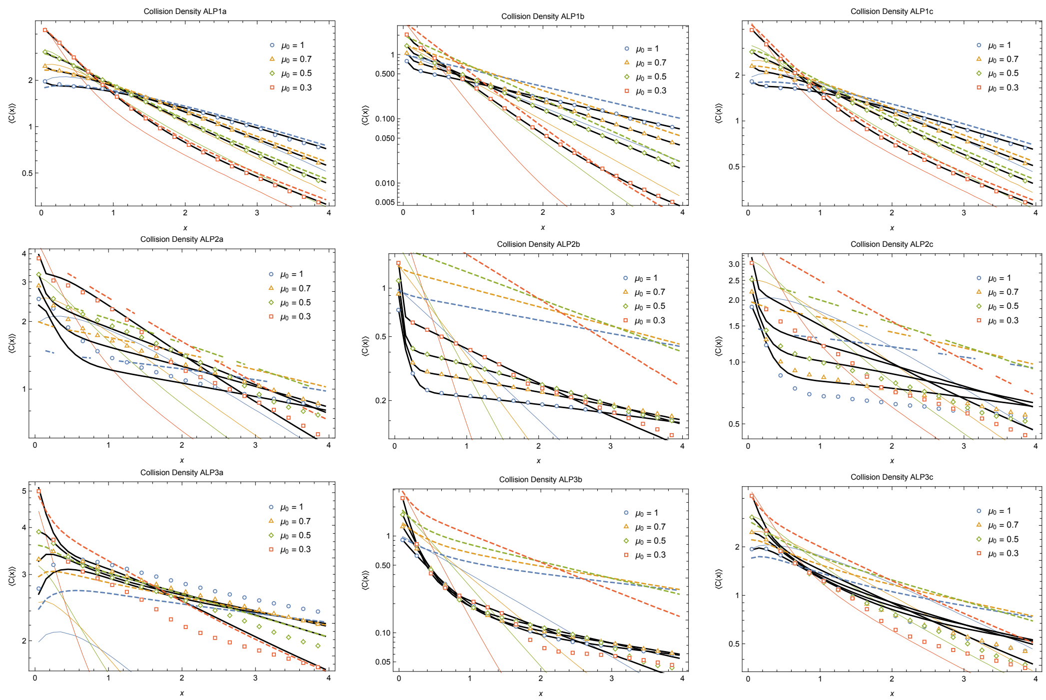

Figure 4: Scalar collision density $C(x)$ at depth x inside the half space—Quenched disorder (markers), CLS (black), GRT (dashed), AM (thin).

Configuration		Benchmark	Annealed: Relative errors			
Case	μ_0	Quenched	CLS	GRT	GRT(non-reciprocal)	Atomic Mix
ALP1a	1.0	0.352004	-2.956%	-0.08236%	23.37%	22.82%
	0.7	0.394946	-1.537%	1.228%	22.62%	22.43%
	0.5	0.434278	-1.063%	1.599%	21.03%	21.05%
	0.3	0.486311	-0.7734%	1.734%	18.54%	18.73%
ALP1b	1.0	0.0286932	-2.9%	-67.15%	-47.46%	-48.43%
	0.7	0.0352121	-2.947%	-67.17%	-47.84%	-48.29%
	0.5	0.0414191	-2.544%	-66.91%	-47.82%	-47.9%
	0.3	0.0505851	-1.941%	-66.24%	-47.55%	-47.26%
ALP1c	1.0	0.3477	-3.416%	-3.67%	19.92%	19.32%
	0.7	0.392428	-2.374%	-2.624%	18.92%	18.69%
	0.5	0.432231	-1.906%	-2.14%	17.52%	17.55%
	0.3	0.484798	-1.541%	-1.77%	15.35%	15.54%
ALP2a	1.0	0.201843	-17%	4.706%	117.8%	114.2%
	0.7	0.219716	-12.49%	11.91%	121.5%	120.1%
	0.5	0.235958	-8.507%	17.96%	122.9%	122.8%
	0.3	0.258986	-3.117%	25.69%	121.7%	122.9%
ALP2b	1.0	0.130098	-12.73%	-96.57%	-87.78%	-88.63%
	0.7	0.155508	-12.48%	-96.51%	-87.87%	-88.29%
	0.5	0.179387	-12.35%	-96.42%	-87.85%	-87.97%
	0.3	0.213368	-12.27%	-96.21%	-87.7%	-87.5%
ALP2c	1.0	0.306495	-24.32%	-35.21%	37.83%	35.36%
	0.7	0.346118	-22.09%	-33.1%	35.58%	34.57%
	0.5	0.381498	-20.21%	-31.13%	33.23%	33.19%
	0.3	0.429897	-17.79%	-28.26%	29.52%	30.3%
ALP3a	1.0	0.678516	-8.392%	-7.427%	12.7%	-36.29%
	0.7	0.711203	-6.254%	-5.346%	11.55%	-32.01%
	0.5	0.734258	-4.177%	-3.206%	11%	-28.41%
	0.3	0.761093	-1.56%	-0.3306%	10.34%	-24.13%
ALP3b	1.0	0.0127678	-26.14%	-92.55%	-86.06%	15.89%
	0.7	0.0157418	-26.2%	-92.64%	-87.04%	15.66%
	0.5	0.0188683	-27.02%	-92.71%	-87.84%	14.37%
	0.3	0.0237585	-28.5%	-92.7%	-88.72%	12.28%
ALP3c	1.0	0.357215	-17.98%	-18.71%	22.56%	16.14%
	0.7	0.397662	-16.27%	-17.04%	19.5%	17.13%
	0.5	0.43311	-14.4%	-15.19%	17.09%	17.32%
	0.3	0.481769	-11.5%	-12.21%	13.88%	16.27%

Table 1: Benchmark values for the total reflectance/albedo (R) and relative errors of approximate annealed disorder models.